

Modified Knudsen ansatz and elliptic flow in $\sqrt{s}=14$ TeV pp collisions

A. K. Chaudhuri*

Variable Energy Cyclotron Centre, 1/AF, Bidhan Nagar, Kolkata 700 064, India

(Dated: February 17, 2022)

Assuming that hot spots are formed in initial pp collisions, in a modified Knudsen ansatz, which accounts for the entropy generation in viscous fluid evolution, we have given predictions for elliptic flow in $\sqrt{s}=14$ TeV pp collisions. Predicted flow depends on the number of hot spots and hot spot sizes. If two to four hot spots of size ≈ 0.1 fm are formed in initial pp collisions, in events with multiplicity $n_{mult} \approx 10-15$, modified Knudsen ansatz predicted flow is accessible experimentally in 4th order cumulant method.

PACS numbers: 25.75.-q, 25.75.Dw, 25.75.Ld

In recent years, there is much interest in elliptic flow in pp collisions at LHC energy. Finite elliptic flow has been observed in $\sqrt{s_{NN}}=200$ GeV Au+Au collisions [1–4] and more recently in $\sqrt{s_{NN}}=2.76$ TeV Pb+Pb collisions [5]. Finite elliptic flow in relativistic heavy ion collisions is regarded as a definitive signature of collective effect [6, 7]. It is also best understood in a collective model like hydrodynamics [8]. In a non-central collision, the reaction zone is spatially asymmetric. Differential pressure gradient convert the spatial asymmetry in to momentum asymmetry. In other words, in a hydrodynamic model, spatial asymmetry ($\varepsilon_x = \frac{\langle y^2 \rangle - \langle x^2 \rangle}{\langle y^2 \rangle + \langle x^2 \rangle}$) of the interaction region controls the elliptic flow. Since protons have finite extension (though of smaller size than a nucleus), in principle, in finite impact parameter pp collisions asymmetric reaction zone can produce elliptic flow. Similarities between pp and Au+Au collisions have been observed even at RHIC energy [9]. When phase space restriction due to conservation laws is taken into account transverse momentum distribution in pp and Au+Au collisions at RHIC energy show similar behavior [9]. However, similarity in p_T spectra alone does not prove that collective model like hydrodynamic is applicable in pp collisions. Observation of finite elliptic flow could be a definitive signature of collective behavior in pp collisions. However, even if flow is produced in pp collisions, whether or not it will be accessible experimentally will depend on both the flow strength and the multiplicity in the phase space window where the flow is measured. This is because non-flow effects like di-jet production, also show azimuthal correlation not related to the reaction plane. They need to be disentangled for faithful reconstruction of the reaction plane. Several standard methods [7, 10–12] have been devised to discriminate non-flow effects. Event plane method [7, 10] determine the reaction plane, but require large multiplicity for unambiguous determination. Cumulant method [11] does not require measurement of the reaction plane. Cumulants of multiparticle azimuthal correlation are related to flow harmonics. The cumulants can be constructed in increasing order ac-

cording to the number of particles that are azimuthally correlated. The method relies on the different multiplicity scaling property of the azimuthal correlation related to flow and non-flow effects. In the cumulant method, for particle multiplicity n_{mult} , v_2 can be reliably extracted using two particle correlator, if $v_2\{2\} > 1/n_{mult}^{1/2}$. Higher order correlators will increase the sensitivity, e.g. $v_2\{4\} > 1/n_{mult}^{3/4}$. Still higher order cumulant (cumulants of order greater than 4) will increase the sensitivity even more, $v_2 > 1/n_{mult}$. In the Lee-Yang zero method [12] elliptic flow is obtained from the zeros in a complex plane of a generating function of azimuthal correlation. It is also less biased by the non-flow correction, $v_2\{Lee - Yang\} > 1/n_{mult}$.

Multiplicity in a pp collision is not large. For example, in the central rapidity region, $|\eta| < 1$, in $\sqrt{s}=7$ TeV pp collisions, ALICE collaboration measured charged particle density $dN_{ch}/d\eta \approx 6$ [13]. If for every charged pair, there is a neutral particle, $n_{mult} \approx 9$ in $\sqrt{s}=7$ TeV pp collisions. Unless the elliptic flow $v_2 > 1/n_{mult}^{3/4} \approx 0.2$, experimentally flow can not be measured in the 4th order cumulant method. In $\sqrt{s}=14$ TeV pp collisions, multiplicity is expected to increase. Extrapolation to existing ALICE data gives $n_{mult} \approx 11$ in $\sqrt{s}=14$ TeV pp collisions. Only $v_2 \geq 0.16$, can possibly be measured. Note that $v_2 \approx 0.16-0.2$ is a very large value. For example, in $\sqrt{s}=2.76$ TeV Pb+Pb collisions, in a peripheral 30-40% collision, in the central rapidity region, multiplicity is ~ 640 and elliptic flow $v_2 \sim 0.08$ [5]. Recently, in [14], $\sqrt{s}=14$ TeV pp collisions were simulated hydrodynamically. The model parameters like initial time, initial energy density distribution, freeze-out temperature were fixed to reproduce expected charged particles multiplicity ($dN/dy \approx 7$) in a minimum bias collision. Elliptic flow as a function of centrality was studied. Even in a peripheral collision, hydrodynamic predictions for v_2 is small, $v_2 < 0.02$. Unless some exotic mechanism is at work, it is unlikely that $v_2 \approx 0.16 - 0.2$ can be generated in pp collisions.

Recently some authors have considered exotic mechanism like hot spot formation in pp collisions at LHC [15],[16],[17]. Elliptic flow is proportional to initial spatial eccentricity. With hot spots, even in a central colli-

*E-mail: akc@veccal.ernet.in

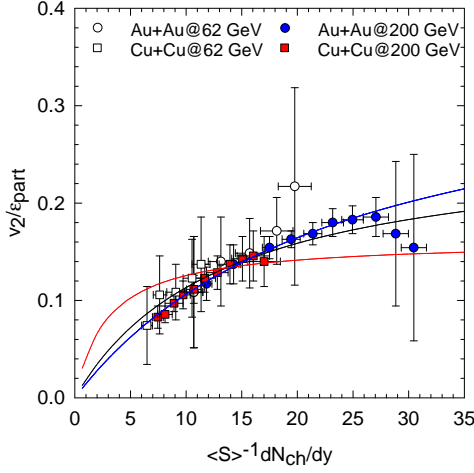


FIG. 1: (color online) PHOBOS data for the centrality dependence of eccentricity scaled elliptic flow in Cu+Cu and Au+Au collisions at $\sqrt{s}=62$ and 200 GeV. The black and red lines are the fit in the unmodified Knudsen ansatz (ideal fluid) with $K_0\sigma c_s=0.05$ and 0.23 respectively. The blue solid and dashed line are the fit in the modified Knudsen ansatz (viscous fluid) with $K_0\sigma c_s=0.05$ and 0.23 respectively.

sion, spatial eccentricity becomes non-zero and measurable elliptic flow can be generated. In [15], it was argued that if 2-3 hot spots are formed in pp collisions, in events with multiplicity $n_{mult} > 50$, experimentally measurable flow can be generated. The widely known Knudsen ansatz [18],

$$\left(\frac{v_2}{\epsilon}\right)^{ex} = \left(\frac{v_2}{\epsilon}\right)^{ih} \frac{\sigma c_s \frac{1}{S} \frac{dN}{dy}}{\frac{1}{K_0} + \sigma c_s \frac{1}{S} \frac{dN}{dy}}, \quad (1)$$

was used to obtain the estimate of elliptic flow in pp collisions. In Eq.1, $\left(\frac{v_2}{\epsilon}\right)^{ih}$ is the hydrodynamic limit for the elliptic flow, S is the transverse area of the reaction zone, σ is the interparticle cross section, c_s is the speed of sound of the medium and K_0 is a non-linear parameter of order ~ 1 , whose exact value can be obtained from explicit transport calculation [19]. $\sigma c_s \frac{1}{S} \frac{dN}{dy}$ can be identified with the inverse Knudsen number, $K^{-1} = \sigma c_s \frac{1}{S} \frac{dN}{dy}$. Eq.1 give qualitatively correct behavior of the experimental elliptic flow. In the limit of small Knudsen number experimental flow approach the ideal hydrodynamic limit $\left(\frac{v_2}{\epsilon}\right)^{ih}$ with a small correction. In the other extreme limit of large Knudsen number, flow is proportional to Knudsen number.

However, Eq.1 is valid only in the ideal fluid approximation. It was obtained with the assumption that the total particle number is conserved throughout the evolution [18]. The assumption is justified in an isentropic expansion, i.e. one dimensional evolution of ideal fluid, when entropy density (s) times the proper time (τ) is a constant. Under such condition, $\frac{1}{S} \frac{dN}{dy} \propto s\tau \approx n\tau$ [20]. However, in a viscous evolution, entropy is generated and

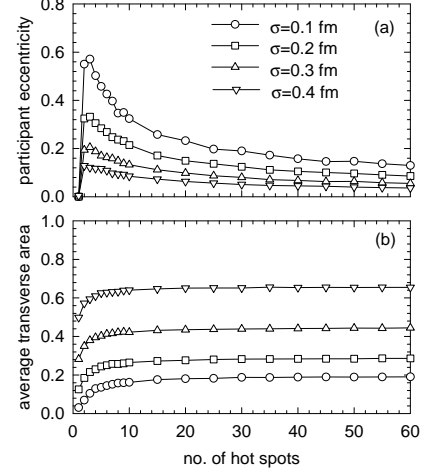


FIG. 2: (a) Variation of event averaged participant eccentricity with hot spot number and size. (b) same for the average transverse area.

initial and final state entropy are not same and the assumption is clearly violated. In [21], Eq.1 was extended to include the effect of entropy generation. In the modified Knudsen ansatz,

$$\left(\frac{v_2}{\epsilon}\right)^{ex} = \left(\frac{v_2}{\epsilon}\right)^{ih} \frac{\frac{1}{S} \frac{dN}{dy} \left[1 + \frac{2}{3\tau_i T_i} \left(\frac{\eta}{s}\right)\right]^{-3}}{\frac{1}{K_0\sigma c_s} + \frac{1}{S} \frac{dN}{dy} \left[1 + \frac{2}{3\tau_i T_i} \left(\frac{\eta}{s}\right)\right]^{-3}} \quad (2)$$

where η/s is the viscosity to entropy ratio of the medium. τ_i and T_i is the initial time and temperature scale. The modified equation clearly brought out the effect of viscosity on elliptic flow. Inverse Knudsen number is reduced, $K^{-1} = \sigma c_s \frac{1}{S} \frac{dN}{dy} \rightarrow \sigma c_s \frac{1}{S} \frac{dN}{dy} \left[1 + \frac{2}{3} \left(\frac{1}{\tau_i T_i} \frac{\eta}{s}\right)\right]^{-3}$. To reproduce the experimental flow, reduction in K^{-1} must be compensated by increase in ideal hydrodynamic limit $\left(\frac{v_2}{\epsilon}\right)^{ih}$. This is an interesting result. Modified Knudsen ansatz require more $\left(\frac{v_2}{\epsilon}\right)^{ih}$ than the unmodified one.

The modified Knudsen ansatz do explains the experimentally observed centrality dependence of elliptic flow. As an example, in Fig.1, fits obtained to the PHOBOS measurements [22–24] for charged particles elliptic flow in $\sqrt{s}=62$ and 200 GeV Au+Au and Cu+Cu collisions are shown. Within the error, PHOBOS measurements of (participant) eccentricity scaled elliptic flow do not show any energy dependence or system size dependence. In the modified Knudsen ansatz, treating $\left(\frac{v_2}{\epsilon}\right)^{ih}$ and $\left(\frac{1}{\tau_i T_i} \frac{\eta}{s}\right)$ as free parameters, we have fitted the PHOBOS data. In the Knudsen ansatz, the combined parameter $K_0\sigma c_s$ needs to be specified. We have used two values, $K_0\sigma c_s=0.05$ and 0.23 to account for the uncertainty in the parameters $c_s = \sqrt{1/3}$, $\sigma=3-4$ mb and $K_0 = 0.7 \pm 0.3$ [19]. The fitted values, along with the χ^2/N of the fit, are listed in table.I. The dashed and solid blue lines in Fig.1 are

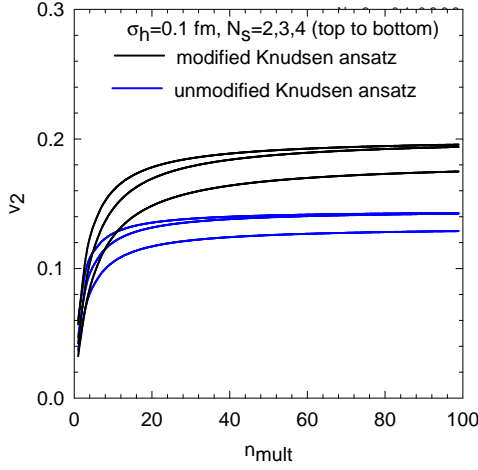


FIG. 3: (color online) Black and blue lines (from top to bottom) are predicted flow in modified and unmodified Knudsen ansatz with $N_s=2, 3$ and 4 hot spots of size 0.1 fm.

the fits obtained with $K_0\sigma c_s=0.05$ and 0.23 respectively. The two fits can not be distinguished. Ideal hydrodynamic limit $(\frac{v_2}{\epsilon})^{ih}=0.36$ is also identical for both the values of $K_0\sigma c_s$. The fitted value of $(\frac{1}{\tau_i T_i} \frac{\eta}{s})$ however differ by a factor of ~ 5 , $(\frac{1}{\tau_i T_i} \frac{\eta}{s})=0.29$ for $K_0\sigma c_s=0.05$ and $(\frac{1}{\tau_i T_i} \frac{\eta}{s})=1.37$ for $K_0\sigma c_s=0.23$. Increase of $(\frac{1}{\tau_i T_i} \frac{\eta}{s})$ with $K_0\sigma c_s$ is also understood. From Eq.2, one immediately gets, $(\frac{v_2}{\epsilon})^{ex} \propto \frac{K_0\sigma c_s}{(\frac{1}{\tau_i T_i} \frac{\eta}{s})}$. Factor of ~ 5 increase in $K_0\sigma c_s$ is compensated by similar increase in $(\frac{1}{\tau_i T_i} \frac{\eta}{s})$.

For comparison, in Fig.1, fits obtained to the PHOBOS data in the unmodified Knudsen ansatz, i.e. without accounting for the entropy generation are also shown. The black and red lines in Fig.1 are the fits obtained in the unmodified Knudsen ansatz respectively for $K_0\sigma c_s=0.05$ and 0.23. The fitted value of $(\frac{v_2}{\epsilon})^{ih}$ are listed in table.I. For both the values of $K_0\sigma c_s$, ideal hydrodynamic limit $(\frac{v_2}{\epsilon})^{ih}$ is less than that obtained in the modified Knudsen ansatz.

If the participant eccentricity and the transverse area are known, results of the analysis of PHOBOS data can be used to predict for elliptic flow in pp collisions. We assume that hot spots are formed in initial pp collisions. They have Gaussian density distribution. For N_s number of hot spots, the energy density of the system can be obtained as,

$$\varepsilon(x, y) = \varepsilon_0 \frac{1}{\sqrt{2\pi\sigma^2}} \sum_{i=1}^{N_s} e^{-\frac{(x-r_i)^2}{2\sigma_h^2}} \quad (3)$$

The centre of the hot spots (\mathbf{r}_i) can be anywhere in the reaction volume. We assume that \mathbf{r}_i 's are randomly distributed within a sphere of radius $R=0.56$ fm. Spatial eccentricity of the reaction zone will depend on the

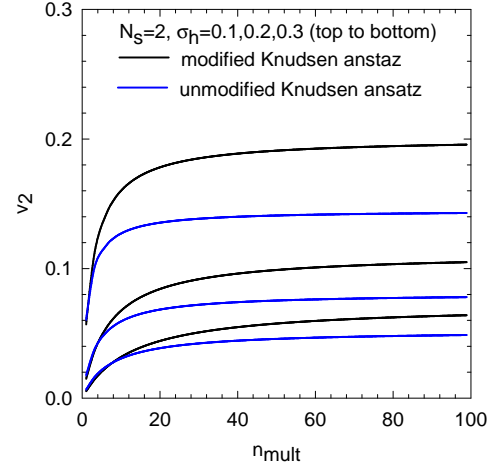


FIG. 4: (color online) Black and blue lines (from top to bottom) are predicted flow in modified and unmodified Knudsen ansatz with two hot spots $N_s=2$, of sizes $\sigma_h=0.1$ fm.

number of hot spots as well as on the size σ_h of the hot spots. In Fig.2, variation average participant eccentricity ($\langle \varepsilon_{part} \rangle$) and transverse area S , with number of hot spots as well as with the size σ_h is shown. To be consistent with PHOBOS measurements, $\langle \varepsilon_{part} \rangle$ and S are computed as follows:

$$\langle \varepsilon_{part} \rangle = \frac{\sqrt{(\sigma_y^2 - \sigma_x^2) + 4\sigma_{xy}^2}}{\sigma_y^2 + \sigma_x^2} \quad (4)$$

$$S = \pi \sqrt{\sigma_x^2 \sigma_y^2 - \sigma_{xy}^2} \quad (5)$$

where $\sigma_x^2 = \langle x^2 \rangle - \langle x \rangle^2$, $\sigma_y^2 = \langle y^2 \rangle - \langle y \rangle^2$ and $\sigma_{xy} = \langle xy \rangle - \langle x \rangle \langle y \rangle$, and $\langle \dots \rangle$ denote energy density weighted averaging.

If a single hot spot is formed, the $\langle \varepsilon_{part} \rangle \approx 0$. $\langle \varepsilon_{part} \rangle$ is maximum if only two hot spots are formed in the initial collisions. $\langle \varepsilon_{part} \rangle$ decreases as more and more hot spots are formed and for very large number of hot spots $\langle \varepsilon_{part} \rangle \rightarrow 0$. $\langle \varepsilon_{part} \rangle$ also decreases with increasing size of the hot spots. Average transverse area (S) increases with N_s and saturates beyond $N_s \approx 5$. S also increases with the hot spot size.

TABLE I: Hydrodynamic limit $(\frac{v_2}{\epsilon})^{ih}$ and time and temperature scaled viscosity to entropy ratio from fit to PHOBOS data. The superscript (*) indicate that the value was kept fixed during fitting.

$K_0\sigma c_s(fm^2)$	$(\frac{v_2}{\epsilon})^{ih}$	$(\frac{1}{\tau_i T_i} \frac{\eta}{s})$	χ^2/N
0.05*	0.36	0.29	0.08
0.23*	0.36	1.37	0.08
0.05*	0.26	0.0*	0.28
0.23*	0.16	0.0*	2.20

Knudsen ansatz predictions for elliptic flow in pp collisions are shown in Fig.3. The blue lines are the predicted

TABLE II: Minimum multiplicity (n_{mult}^{min}) beyond which modified Knudsen ansatz predictions for v_2 is accessible in 4th and 2nd order cumulant method are given as a function of hot spot numbers (N_s) and hot spot size σ (in fm). The bracketed numbers are the same in the unmodified Knudsen ansatz.

N_s	n_{mult}^{min} in 4th order cumulant			n_{mult}^{min} in 2nd order cumulant		
	$\sigma = 0.1$	$\sigma = 0.2$	$\sigma = 0.3$	$\sigma = 0.1$	$\sigma = 0.2$	$\sigma = 0.3$
2	12 (15)	23 (29)	48 (63)	30 (51)	76 (> 100)	> 100 (> 100)
3	13 (16)	25 (32)	47 (60)	32 (52)	86 (> 100)	> 100 (> 100)
4	15 (18)	28 (35)	48 (62)	38 (63)	96 (> 100)	> 100 (> 100)

flow in the unmodified Knudsen ansatz, i.e. in the ideal fluid approximation, with two, three and four hot spots in the initial state. Hot spot size is assumed to be $\sigma_h=0.1$ fm. The predictions are obtained for $K_0\sigma c_s=0.05$. Depending on the number of hot spots, at large multiplicity predicted flow varies between 0.12-0.14. The black lines in Fig.3 are the predicted flow in the modified Knudsen ansatz. The modified Knudsen ansatz predicts $\sim 30\%$ more flow. We may note that if $K_0\sigma c_s=0.23$, instead of 0.05 is used, while the flow will remain unchanged in the modified Knudsen ansatz, the unmodified Knudsen ansatz will predict $\sim 40\%$ less flow.

In Fig.4, Knudsen ansatz predictions for flow, as a function of the hot spot size are shown. Number of hot spots in the initial collisions is assumed to be two.

Predicted flow decreases with increasing hot spot size. For hot spot sizes 0.1, 0.2 and 0.3 fm, in the unmodified Knudsen ansatz, at large multiplicity, $v_2 \sim 0.14, 0.08, 0.05$ respectively. Modified Knudsen ansatz predicts $\sim 30\%$ more flow, $v_2 \sim 0.2, 0.1, 0.06$.

Is the predicted flow is sufficiently strong to be observed experimentally? As noted earlier, in 2nd and 4th order cumulant method, flow is measurable if $v_2\{2\} \geq 1/n_{mult}^{1/2}$ and $v_2\{4\} \geq 1/n_{mult}^{3/4}$. In table.II, the minimum multiplicity n_{mult}^{min} beyond which Knudsen ansatz predicted flow become accessible in 4th and 2nd order cumulant method are noted. For 2-4 hot spots of size $\sigma_h=0.1$ fm, in 4th order cumulant method, modified Knudsen ansatz predicted flows are accessible beyond $n_{mult}^{min}=12-15$. If hot spot sizes are large, flow is accessible only at larger multiplicity. Limiting multiplicity is substantially larger in 2nd cumulant method, $n_{mult}^{min}=30-38$, for 2-4 hot spots of size 0.1 fm. Unmodified Knudsen ansatz predicts less flow and demand higher multiplicity events for detection.

To summarise, assuming that hot spot like structures are formed in pp collisions, in a modified Knudsen ansatz, which accounts for the entropy generation in viscous evolution, we have given predictions for the centrality dependence of elliptic flow in $\sqrt{s}=14$ TeV pp collision at LHC. Predicted flow depends on the number of hot spots as well as on the hot spot sizes. For 2-4 hot spots of size 0.1 fm, in large multiplicity events, modified Knudsen ansatz predicts $v_2 \approx 0.18-0.20$. Even in low multiplicity, $n_{mult} \approx 10-15$, events, predicted flow could be measured experimentally in 4th order cumulant method.

-
- | | |
|---|---|
| <p>[1] BRAHMS Collaboration, I. Arsene <i>et al.</i>, Nucl. Phys. A 757, 1 (2005).</p> <p>[2] PHOBOS Collaboration, B. B. Back <i>et al.</i>, Nucl. Phys. A 757, 28 (2005).</p> <p>[3] PHENIX Collaboration, K. Adcox <i>et al.</i>, Nucl. Phys. A 757 184 (2005).</p> <p>[4] STAR Collaboration, J. Adams <i>et al.</i>, Nucl. Phys. A 757 102 (2005).</p> <p>[5] K. Aamodt <i>et al.</i> [The ALICE Collaboration], arXiv:1011.3914 [nucl-ex].</p> <p>[6] J. Y. Ollitrault, Phys. Rev. D 46, 229 (1992).</p> <p>[7] A. M. Poskanzer and S. A. Voloshin, Phys. Rev. C 58, 1671 (1998)</p> <p>[8] P. F. Kolb and U. Heinz, in <i>Quark-Gluon Plasma 3</i>, edited by R. C. Hwa and X.-N. Wang (World Scientific, Singapore, 2004), p. 634.</p> <p>[9] Z. Chajecki and M. Lisa, Nucl. Phys. A 830, 199C (2009)</p> <p>[10] J. Y. Ollitrault, Phys. Rev. D 48, 1132 (1993)</p> <p>[11] N. Borghini, P. M. Dinh and J. Y. Ollitrault, Phys. Rev. C 64, 054901 (2001)</p> <p>[12] R. S. Bhalerao, N. Borghini and J. Y. Ollitrault, Nucl. Phys. A 727, 373 (2003) [arXiv:nucl-th/0310016].</p> <p>[13] K. Aamodt <i>et al.</i> [ALICE Collaboration], Eur. Phys. J. C 68, 345 (2010) [arXiv:1004.3514 [hep-ex]].</p> | <p>[14] S. K. Prasad, V. Roy, S. Chattopadhyay and A. K. Chaudhuri, arXiv:0910.4844 [nucl-th].</p> <p>[15] J. Casalderrey-Solana and U. A. Wiedemann, Phys. Rev. Lett. 104, 102301 (2010) [arXiv:0911.4400 [hep-ph]].</p> <p>[16] P. Bozek, arXiv:0911.2392 [nucl-th].</p> <p>[17] A. K. Chaudhuri, Phys. Lett. B 692, 15 (2010) [arXiv:0912.2578 [nucl-th]].</p> <p>[18] R. S. Bhalerao, J. P. Blaizot, N. Borghini and J. Y. Ollitrault, Phys. Lett. B 627, 49 (2005) [arXiv:nucl-th/0508009].</p> <p>[19] C. Gombeaud and J. Y. Ollitrault, Phys. Rev. C 77, 054904 (2008) [arXiv:nucl-th/0702075].</p> <p>[20] R. C. Hwa and K. Kajantie, Phys. Rev. D 32, 1109 (1985).</p> <p>[21] A. K. Chaudhuri, Phys. Rev. C 82, 047901 (2010) [arXiv:1006.4478 [nucl-th]].</p> <p>[22] B. B. Back <i>et al.</i> [PHOBOS Collaboration], Phys. Rev. C 72, 051901 (2005) [arXiv:nucl-ex/0407012].</p> <p>[23] B. Alver <i>et al.</i> [PHOBOS Collaboration], Phys. Rev. Lett. 98, 242302 (2007) [arXiv:nucl-ex/0610037].</p> <p>[24] B. Alver <i>et al.</i>, Phys. Rev. C 77, 014906 (2008) [arXiv:0711.3724 [nucl-ex]].</p> |
|---|---|